Effect of Zirconium and Cerium Loadings on Aerogel Pd-Based Catalysts for Methane Combustion

Khouloud Sadouki, Shemseddine Fessi, Zouhaier Ksibi, Mickael Capron, Franck Dumeignil, Abdelhamid Ghorbel

Scientific Research Publishing

Advances in Materials Physics and Chemistry, 2018, 8, 105-119
http://www.scirp.org/journal/ampc
ISSN Online: 2162-5328
ISSN Print: 2162-531X

Effect of Zirconium and Cerium Loadings on Aerogel Pd-Based Catalysts for Methane Combustion

Khouloud Sadouki[1], Shemseddine Fessi[1,2], Zouhaier Ksibi[1], Mickael Capron[3], Franck Dumeignil[3], Abdelhamid Ghorbel[1]

[1]Laboratoire de Chimie des Matériaux et Catalyse, Département de Chimie, Faculté des Sciences de Tunis, Université Tunis-El Manar, Campus Universitaire, Tunis, Tunisie
[2]Chemistry Department, Faculty of Science and Arts, University of Jeddah, Jeddah, Saudi Arabia
[3]Univ. Lille, CNRS, Centrale Lille, ENSCL, Univ. Artois, UMR 8181-UCCS-Unité de Catalyse et Chimie du Solide, Lille, France
Email: khouloud.sadouki21@gmail.com

How to cite this paper: Sadouki, K., Fessi, S., Ksibi, Z., Capron, M., Dumeignil, F. and Ghorbel, A. (2018) Effect of Zirconium and Cerium Loadings on Aerogel Pd-Based Catalysts for Methane Combustion. *Advances in Materials Physics and Chemistry*, **8**, 105-119.
https://doi.org/10.4236/ampc.2018.83008

Received: November 8, 2017
Accepted: March 13, 2018
Published: March 16, 2018

Abstract

Aerogel Pd/($Ce_{0.33}Zr_{0.66}O_2$)SiO_2 catalysts (CeZry) were prepared with variable Ce and Zr loadings (molar ratio Ce/Zr = 1/2) by combining sol-gel and impregnation methods. First, N_2-physisorption was used to investigate the texture evolution. Then, H_2-chimisorption and TEM were performed to study the effect on particle dispersion. After, TPR was used to determine the catalyst reducibility. Furthermore, XPS characterization was done to identify the palladium oxidation state and to evaluate the Pd-support interaction. Finally, the prepared catalysts were tested in methane combustion to assess their catalytic activity. The obtained results showed that, when the Zr and Ce loadings are varied between 0% and 8% and between 0% and 6% respectively, the BET surface area was increased from 615 to 744 m^2/g, the porosity diameter from 45.7 to 83.6 Å, the Pd particle diameter from 5.2 to 7.0 nm, the CeO_2 and ZrO_2 particle size from 0 to 68 nm, the reduction temperature shift reached 16˚C, the Pd binding energy shift attained 0.6 eV, but an optimum amounts of Zr (4 wt.%) and Ce (3 wt.%) are needed to maximize the PdO reducibility and to enhance the catalytic activity. In effect, 100% conversion of methane was reached at around 415˚C on the CeZr4 catalyst.

Keywords

Pd/($CexZr_{(1-x)}O_2$)/SiO_2 Catalysts, Methane Combustion, Catalytic Activity

1. Introduction

Methane is an economical and clean alternative to fuels; it is used to produce energy in gas turbine combustors and as a new energy for vehicles [1]. The advantage of catalytic combustion of methane is that operates at much lower temperatures than flame combustion, which greatly reduces the noxious emissions of nitrogen oxides, NO_x and unburned hydrocarbons [2]. Palladium oxide is considered to be an effective catalyst in methane oxidation [3] [4] [5] [6]. Unfortunately, the deactivation of the catalyst due to the sintering of palladium during heat treatments is a serious problem for this kind of catalysts [7]. Therefore, it is necessary to modify the Pd-base catalysts to improve their thermal stability. Among the parameter which may affect the thermal stability of the catalyst are the support and the additives [8]. The ceria-zirconia-supported palladium catalysts showed high activity [9] [10] due to CeO_2-ZrO_2 redox properties and oxygen storage capacity (OSC) which is better than pure CeO_2 [9] [10] [11] [12]. The addition of zirconium into the cubic CeO_2 framework is effective to prevent cerium sintering, to improve the oxygen mobility in the lattice and to increase thermal stability [13]. Furthermore, the use of SiO_2 as a support could promote OSC because of its relatively higher dispersive properties due to its relatively high surface area, and because its relatively inert character compared to other supports [14], which prevent CeO_2 depletion through, e.g., reaction with the support giving compounds such as $CeAlO_3$ formation causing the OSC decrease when Al_2O_3 is used [15]. However, studies on aerogel SiO_2 as a support for $Ce_xZr_{1-x}O_2$ oxide have been scarcely reported, especially when concerning the effect of $Ce_xZr_{1-x}O_2$ loading on the Pd/($Ce_xZr_{1-x}O_2$)SiO_2 catalyst for methane combustion. For these reasons, in the research presented herein, the sol-gel process was used to prepare a SiO_2 aerogel known to have a relatively high specific surface area, which enables relatively better dispersion of cerium and zirconium oxides and lower thickness of the pore walls, which increase oxygen mobility [17]. However appropriate amounts of Ce and Zr are needed to make the modification efficient [16]. The impregnation method was then used to add palladium and to prepare the Pd/($Ce_{0.33}Zr_{0.66}O_2$)SiO_2 catalysts. The effect of Ce and Zr loadings on the texture, the structure and the catalytic activity in methane combustion was then studied.

2. Experimental

2.1. Chemicals

Cerium nitrate $Ce(NO_3)_3{\cdot}6H_2O$ (Sigma-Aldrich, 99.99%), zirconium(IV) oxynitrate hydrate $ZrO(NO_3)_3{\cdot}xH_2O$ (Sigma-Aldrich, 99.99%), ethanol C_2H_5OH (Sigma-Aldrich, ≥99.8%), tetraethyl orthosilicate $Si(OC_2H_5)_4$ (TEOS) (ACROS, 98%), acetic acid CH_3COOH (Sigma-Aldrich, ≥99.7%) and palladium acetate ($Pd(OAc)_2$) (Fluka, 35.5% Pd) are used as chemicals in this work.

2.2. Support Preparation

The $(Ce_{0.33}Zr_{0.66}O_2)SiO_2$ support was prepared by sol-gel method with variable Ce and Zr loadings (Zr % = 0, 2, 4 and 8 wt.%) and a fixed molar ratio Zr/Ce = 2. $Ce(NO_3)_3{\cdot}6H_2O$, $ZrO(NO_3)_3{\cdot}xH_2O$, CH_3COOH, $Si(OC_2H_5)_4$(TEOS), ethanol and deionized water were mixed at 40˚C. The molar ratios of H_2O/TEOS = 15 and CH_3COOH/TEOS = 1. The obtained sol was maintained under constant stirring until a spongy and transparent gel was formed. The solvent was then removed by evaporation under supercritical conditions of ethanol (T_c = 240.9˚C, P_c = 6.14 MPa). Finally, the obtained solid was calcined at 550˚C for 4 h under oxygen flow (30 mL/min).

2.3. Catalyst Preparation

The $Pd/(Ce_{0.33}Zr_{0.66}O_2)SiO_2$ catalysts (CeZry, where y is the Zr loading) were prepared by the impregnation method. The appropriate amounts of palladium acetate and $(Ce_{0.33}Zr_{0.66}O_2)SiO_2$ solid were ground in an agate mortar for 10 min. The chosen loading of Pd was 0.5 wt.%. Then, acetone was added (1 mL/g) to obtain a paste which was dried at 60˚C and calcined at 550˚C for 2 h under oxygen flow (30 mL/min).

2.4. Catalyst Characterization

The BET specific surface area and the average pore diameter were determined from N_2 adsorption-desorption measurements using an automatic Micrometrics ASAP 2020 device (error percentage: 5%). Hydrogen chemisorption measurements were performed at 100˚C in a Micromeritics ASAP 2020C equipment after an in-situ reduction treatment under hydrogen at 300˚C for 2 h. Temperature programmed reduction (TPR) was performed with H_2 using a quartz U-tube reactor, coupled to a thermal conductivity detector (TCD). The catalyst (0.05 g) was dried at 250˚C during 0.5 h under argon flow (AGA, 99.99%) and reduced with 10 v/v % H_2/Ar flow (30 ml/min) from 25˚C to 400˚C (10˚C/min). TEM studies were performed on a TECNAI G2 instrument operating at 200 kV (error percentage: 2%). The XPS analyses were conducted on calcined samples using a Kratos Analytical AXIS UltraDLD spectrometer (the error percentage was below 1%). The catalytic activity for methane combustion was determined over the calcined sample (0.1 g) in a dynamic micro-reactor.

A flow comprising 1 vol.% methane, 4 vol.% oxygen and balanced with helium was mixed and regulated at a total flow of 100 mL/min. The reactor effluent was then analyzed by a thermal conductivity detector at different reaction temperatures.

The methane conversion and the turnover frequencies (TOF) were calculated by the following equations:

$$\text{Conversion}(\%) = \frac{P_{CO_2}}{P_{CH_4} + P_{CO_2}} \times 100$$

P_{CH_4} and P_{CO_2} are respectively, the partial pressures of methane and carbon dioxide.

$$TOF = \frac{A \times M_{Pd}}{l \times D}$$

$$A = \frac{P_{CO_2} \times D_T \times 273}{22.4 \times T_r \times m}$$

A: catalyst activity (%), M_{Pd}: atomic mass of palladium (106.42 g/mol), l: Pd loading (wt%), D_T: total gas flow (L/h), T_r: room temperature, m: catalyst weight (g) and D the dispersion (%).

3. Results and Discussion

3.1. Nitrogen Physisorption

The N_2-physisorption results of the Pd/$(Ce_{0.33}Zr_{0.66}O_2)SiO_2$ catalysts summarized in Table 1 show that the textural properties of the solids were significantly modified when the Ce and Zr loadings were increased. Indeed, the pore volume varied between 0.83 and 1.68 cm^3/g, the average pore diameter between 45.7 and 83.6 Å and the BET specific surface area between 615 and 744 m^2/g, (see Table 1). As can be noted, the surface area of Pd/$(Ce_{0.33}Zr_{0.66}O_2)SiO_2$ was larger than that of Pd/SiO_2. These results showed that there is an interaction between CeO_2-ZrO_2 and SiO_2, which resulted in an increase in surface area of support, similar phenomenon has been observed in the literature [17]. Which suggest that this interaction can enhance also the thermal stability of palladium supported catalysts. In addition, it is important to note, that all the adsorption-desorption isotherms were of type IV in the BDDT classification (Figure 1) and that hysteresis loops apparent on the all isotherms was identified as being of the H1 type (IUPAC), which is characteristic of cylindrical pores. These results suggest that the preparation method adopted in this work is able to produce mesoporous ceria-zirconia-silica supports with improved surface area when the Ce and Zr contents increase. In the present work, 8% of Zr and 6% of Ce allows yielding a Pd/$(Ce_{0.33}Zr_{0.66}O_2)SiO_2$ catalyst with a relatively high surface area equal to 744 m^2/g.

Table 1. Zr and Ce weight contents, BET surface area S_{BET} (m^2/g), average pore diameter Dp (Å), total pore volume Vp (cm^3/g), Pd dispersion D_{H2} (%), average Pd particle diameter d_{H2} and average CeO_2-ZrO_2 particle diameter d_{TEM} of the Pd/$(Ce_{0.33}Zr_{0.66}O_2)SiO_2$ catalysts.

Sample	Zr wt.%	Ce wt.%	S_{BET}[a] m^2/g	Dp[a] (Å)	Vp[b] (cm^3/g)	D_{H2}[c] (%)	d_{H2}(Pd)[c] (nm)	d_{TEM}(CeO_2-ZrO_2)[d] (nm)
CeZr8	8	6	744	58.9	1.13	18	5.2	68
CeZr4	4	3	734	83.6	1.68	17	5.6	32
CeZr2	2	1.5	696	60.6	1.18	16	5.7	12
CeZr0	0	0	615	45.7	0.83	14	7.0	-

[a]From N_2 chemisorption at 77 K using the BET equation. [b]Total pore volume estimated at reduced pressure $P/P_0 = 0.99$, accuracy ± 0.01 cm^3/g. [c]Based on H_2 chemisorption measurements. [d]Estimated according to the TEM images.

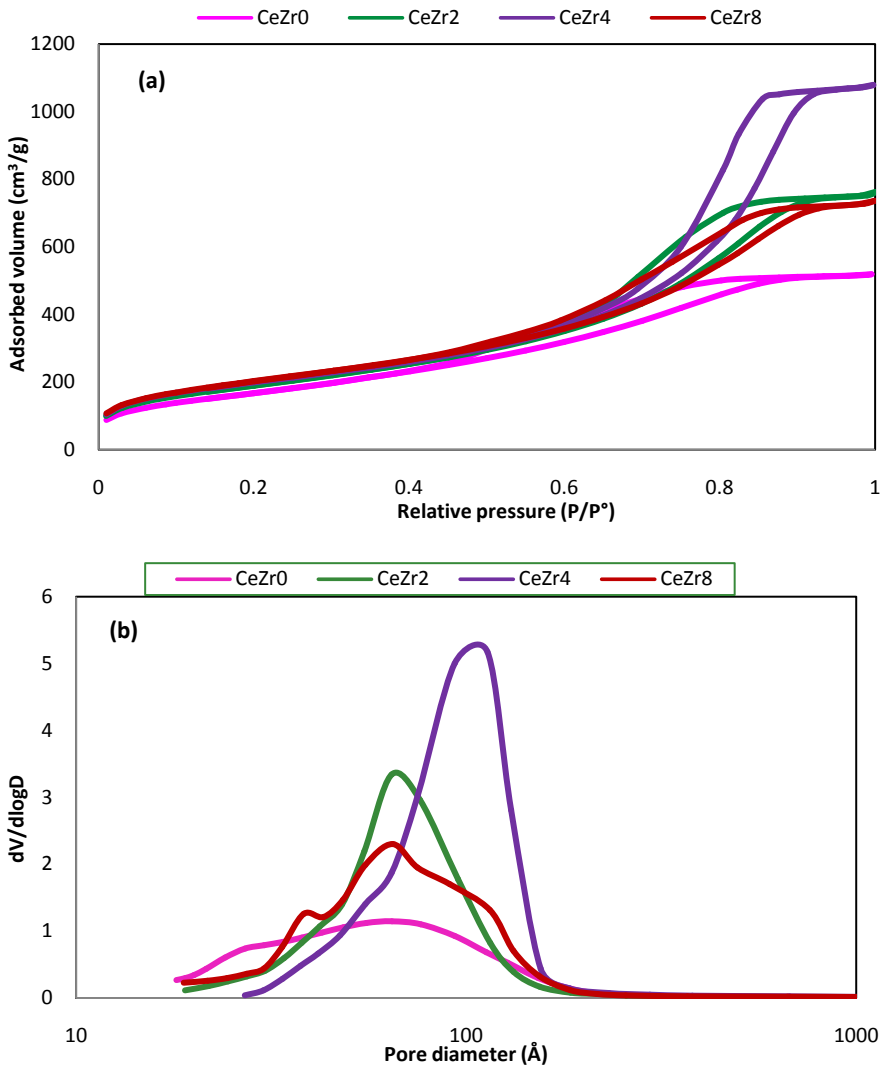

Figure 1. (a) Effect of the Zr and Ce loadings on the adsorption-desorption isotherm profile of the Pd/($Ce_{0.33}Zr_{0.66}O_2$)SiO_2 samples. (b) Average pore diameter distributions of the Pd/($Ce_{0.33}Zr_{0.66}O_2$)SiO_2 samples.

Furthermore, we can note that the average pore diameter (Dp) and the total pore volume (Vp) increase with the Ce and Zr loadings up to the CeZr4 catalyst, and then decrease on the CeZr8 sample. The highest Dp and Vp values obtained on the CeZr4 catalyst may affect the catalytic activity through the improvement of the matter and heat transfer limitations.

3.2. Hydrogen Chemisorption

The hydrogen chemisorption analyses were conducted on the Pd/($Ce_{0.33}Zr_{0.66}O_2$)SiO_2 in order to determine the dispersion and the particle sizes of palladium. The obtained results gathered in Table 1, show that the palladium dispersion was slightly improved when the Zr and Ce loadings increased (see Table 1). Indeed, the palladium dispersion increased from 14% on the CeZr0 sample to 18 % on the CeZr8 catalyst. These results suggest that the Pd dispersion could be im-

proved by the increasing the ceria-zirconia amounts [18], According to the previous work in our research group [13], this results explained by the sintering inhibition of the PdO particles. This improvement of thermal stability could be favored by the enhancement of the PdO-support interaction. In our work, the Zr and Ce loadings seem to be insufficient to improve significantly the Pd dispersion.

3.3. TEM Characterization

The TEM images of the Pd/($Ce_{0.33}Zr_{0.66}O_2$)SiO_2 samples are shown in Figure 2. Homogeneous distribution of the Pd particle size and a good dispersion of the

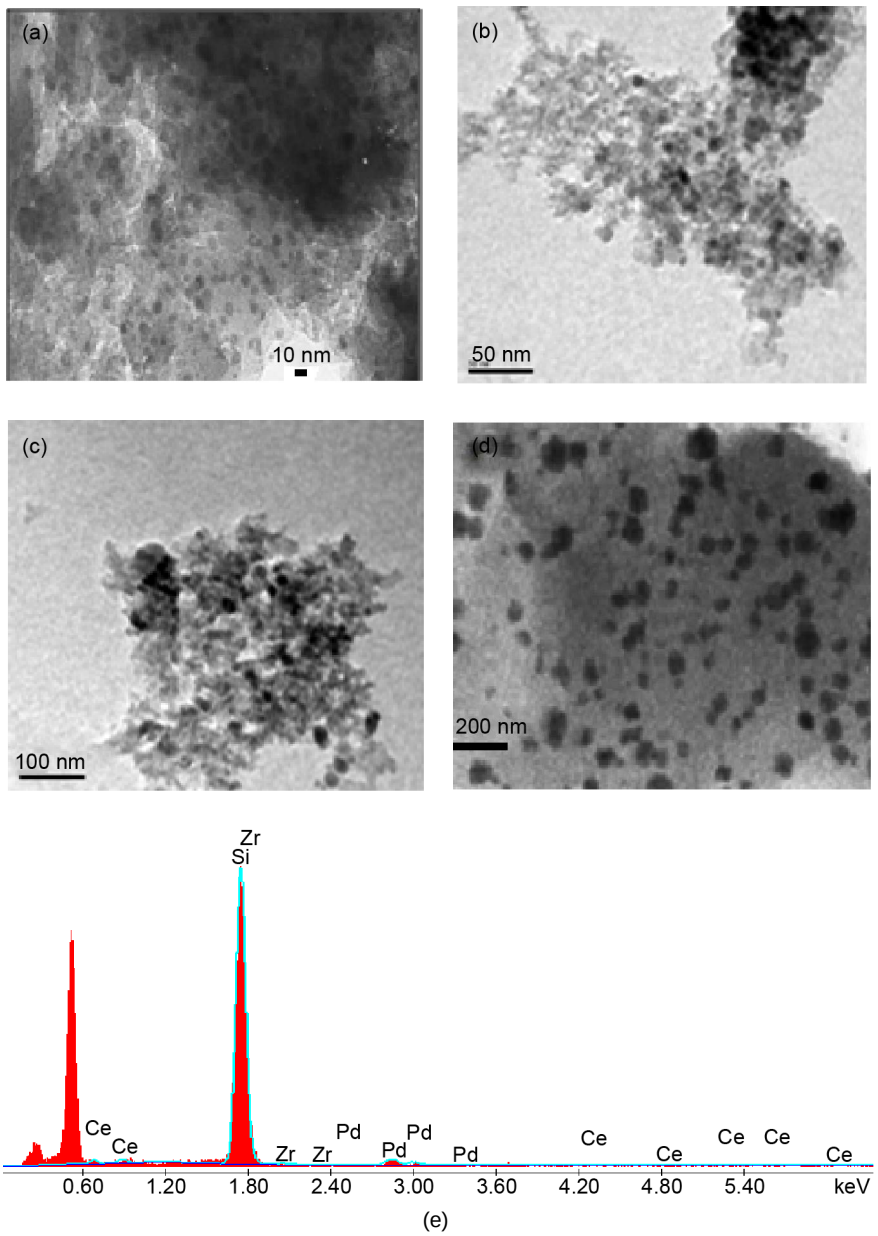

Figure 2. TEM images of the CeZr0 (a), CeZr2 (b), CeZr4 (c), CeZr8 (d) and EDXA of the CeZr4 catalysts (e).

palladium particles are shown on CeZr0 micrograph. According to the particle size distribution, the average Pd particle size is about 6.9 ± 2 nm (**Figure 2(a)**), which in a good agreement with data obtained from hydrogen chemisorption results. For the CeZr2 CeZr4 and CeZr8 micrographs, it is found therein that the morphologies of these catalysts are similar with each other. A careful inspection reveals the existence of crystals with different sizes, dispersed over an amorphous matrix with different contrasts. The average particle sizes of these crystals are respectively about 12, 32 and 68 nm. It is very difficult to know if the observed contrast is associated to CeO_2, ZrO_2 or PdO particles, the accurate measurement of the particle size of Pd cannot be achieved [19]. Ye Yuan *et al.* [20] indicated that most of the Pd particles on a CeO_2 support could not be observed even when HR-TEM was utilized. But according to the chemisorption results the Pd particle size did not exceed 7 nm, which does not make such particles visible on the TEM images. For this reason, the CeO_2 and ZrO_2 identification can be based on their particle growth. Contrarily, to the Pd particles which are more dispersed. These results are in agreement with those of Y. T. Kim *et al.* [21]. The existence of palladium particles is confirmed by EDX analysis (**Figure 2(e)**), which confirms the existence of Pd, Ce and Zr. This result suggests that metallic oxides are well dispersed [13].

3.4. XPS

XPS results indicated that palladium is only present as PdO(Pd^{2+}) species for all catalysts. The $Pd3d_{5/2}$ binding energies for the all Pd/($Ce_{0.33}Zr_{0.66}O_2$) SiO_2 catalysts fall in the range of 336.4 - 337.0 eV (**Table 2**). Generally, the $Pd3d_{5/2}$ binding energy for Pd^0 and Pd^{2+} are about 334.9 ± 0.1 eV and 336.4 ± 0.1 eV, respectively [19]. Here, the $Pd3d_{5/2}$ binding energies on CeZr8 CeZr4, CeZr2 and CeZr0 samples are respectively 336.8, 337.0, 336.5 and 336.4 eV (**Figure 3**). According to the literature, values between 336.8 and 337.0 eV are slightly too high for indicating the presence of pure PdO(Pd^{2+}, 336.4 ± 0.1eV). This increase can be related to the interaction between PdO and the CeZr-O_2/SiO_2 support [16]. Furthermore, the relatively high $Pd3d_{5/2}$ BE on the CeZr4 catalysts (337.0 eV) indicates that optimum amounts of Zr(4 wt.%) and Ce(3 wt.%) are needed to enhance the interaction between Pd species and the support. According to the XPS results, no Pd^0 is detected on catalyst surface. Ciuparu *et al.* [22], explained

Table 2. Pd binding energies and surface atomic composition of the Pd/($Ce_{0.33}Zr_{0.66}O_2$) SiO_2 catalysts.

Sample	BE Pd $3d_{3/2}$ (eV)	BE Pd $3d_{5/2}$ (eV)	Oxidation state	Pd (%)
CeZr8	342.1	336.8	Pd^{2+}	0.02
CeZr4	342.3	337.0	Pd^{2+}	0.02
CeZr2	341.4	336.5	Pd^{2+}	0.02
CeZr0	341.4	336.4	Pd^{2+}	0.02

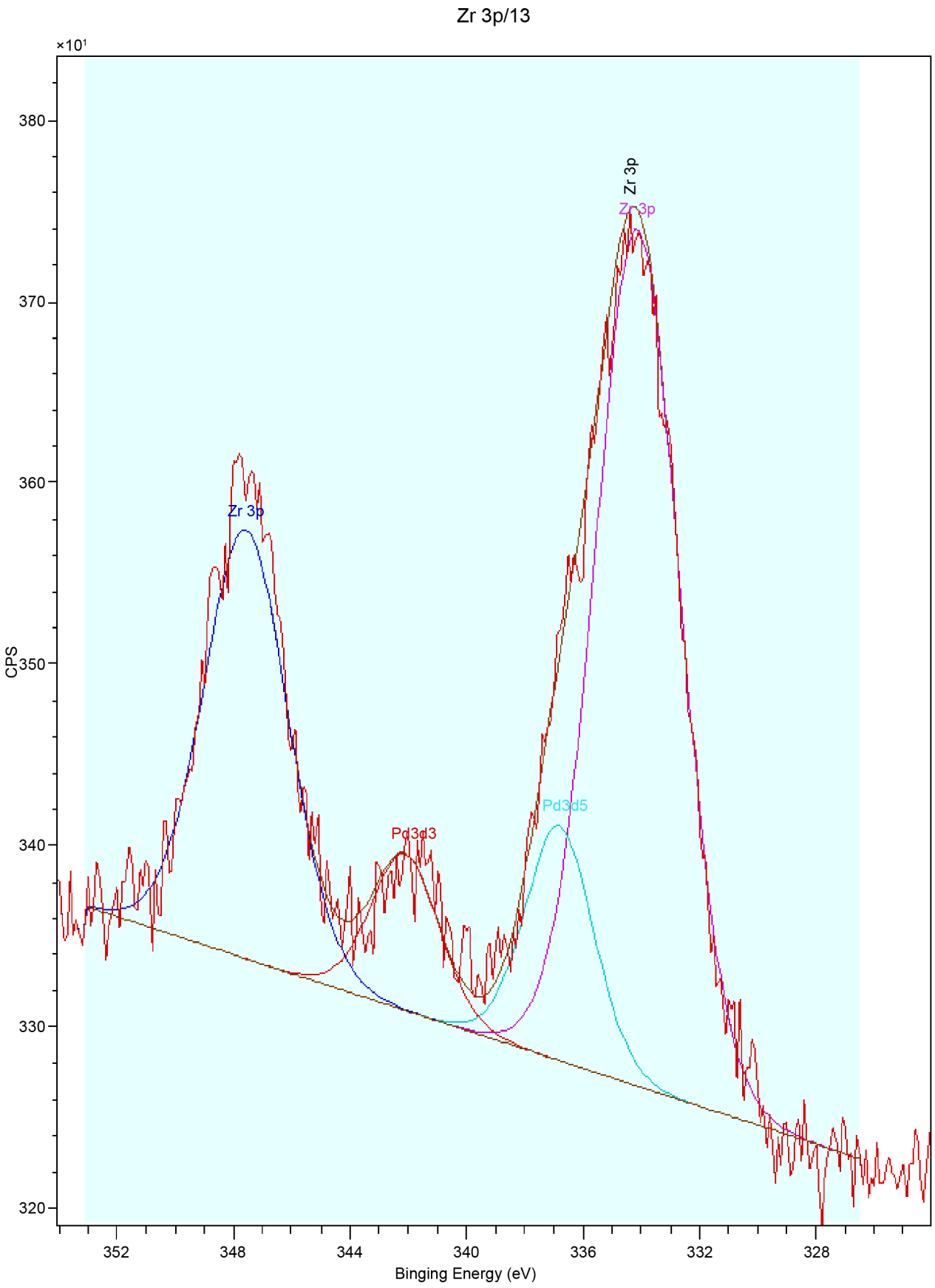
Zr 3p/13
×10¹
380
370
360
350
340
330
320
CPS
Zr 3p
Zr 3p
Zr 3p
Pd3d3
Pd3d5
352
348
344
340
336
332
328
Binging Energy (eV)

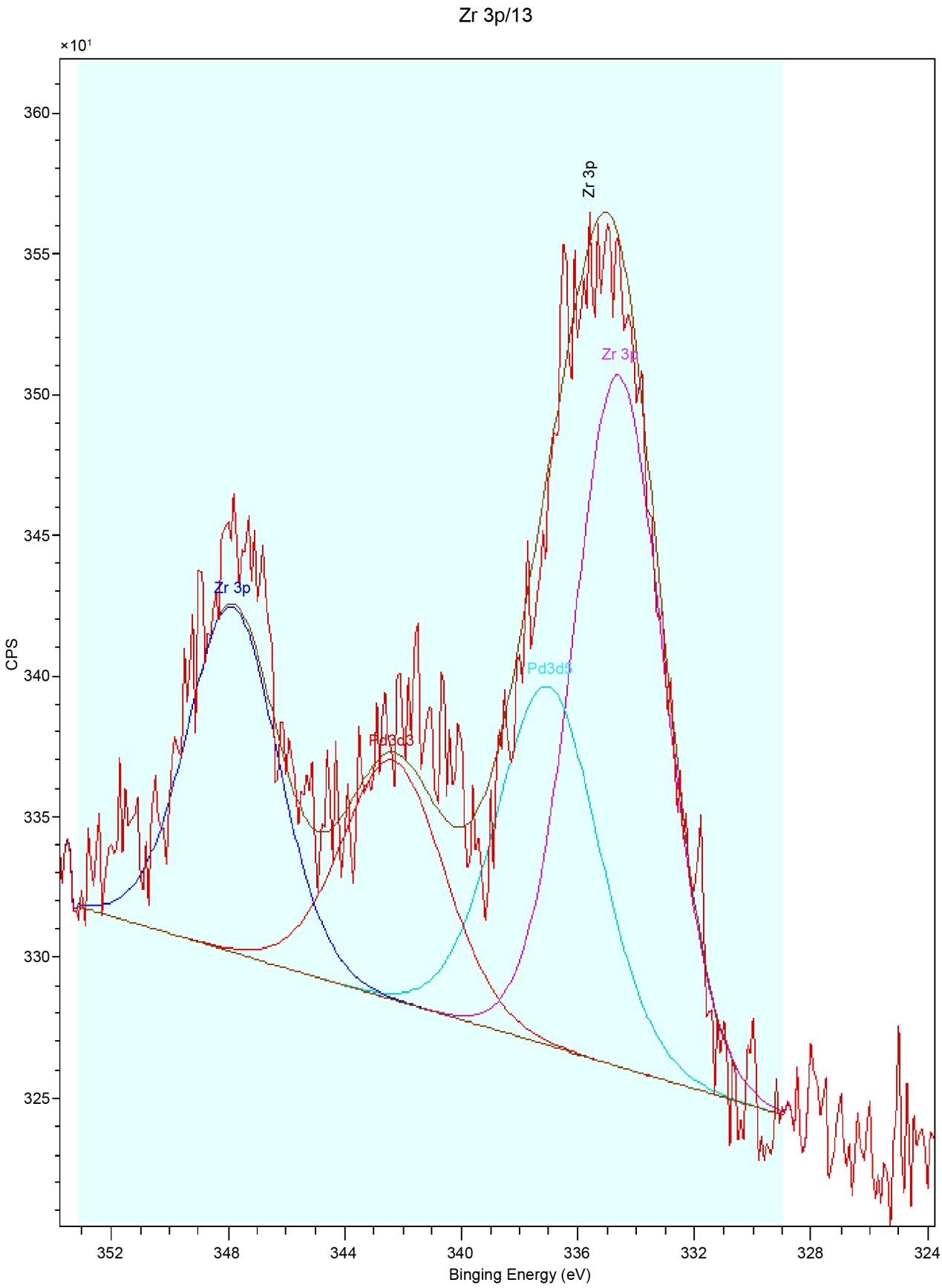
Zr 3p/13
×10¹
360
355
350
345
340
335
330
325
CPS
Zr 3p
Zr 3p
Zr 3p
Pd3d3
Pd3d3
352
348
344
340
336
332
328
324
Binging Energy (eV)

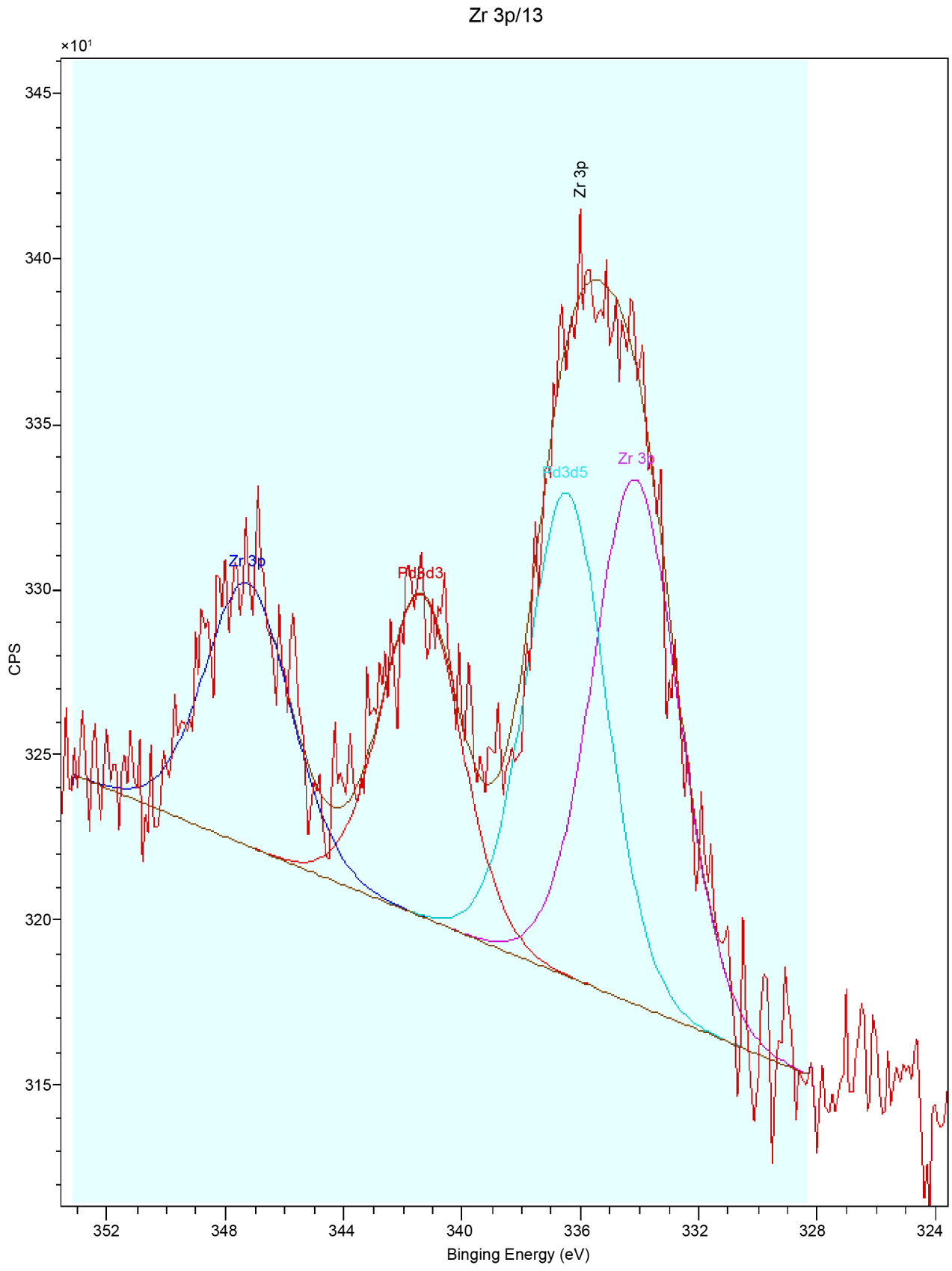

Figure 3. XPS patterns of the Pd/($Ce_{0.33}Zr_{0.66}O_2$)SiO_2 catalysts: (a) CeZr2, (b) CeZr4 and (c) CeZr8.

this result by the phase with lower surface tension tends to encapsulate the phase with higher surface tension. Knowing that oxides have lower surface tension than metals, so the absence of metallic Pd contribution may be explained encapsulated by PdO oxides.

Furthermore, it is important to note that the surface loadings of palladium remains quasi-constant (about 0.02%) with the increase of Ce and Zr amount.

3.5. TPR

The TPR profiles of the Pd/($Ce_{0.33}Zr_{0.66}O_2$)SiO_2 catalyst are shown in **Figure 4**. The negative signals observed below 50˚C, designated as peak α and peak β correspond respectively to the reduction of the larger PdO species dispersed on the catalyst surface and to the reduction of the smaller PdO species having higher interaction with the support [19] [23]. Therefore, they are more stable than the larger PdO species. However, the positive signal, designated as peak γ is attributed to the decomposition of the PdHx species formed during the PdO reduction [23]. According to the obtained results (**Table 3**), the introduction of Zr and Ce on the Pd/SiO_2 catalyst affects the PdOx reducibility. This reducibility increased in the following order: CeZr0 < CeZr8 < CeZr2 < CeZr4. Consequently, the introduction of ceria and zirconia improved the PdO redox property [24]. However, an optimum amounts equal to 4 wt.% of Zr and 3 wt.% of Ce are needed to maximize the PdO reducibility which is a key factor determining the oxidation performance of Pd-based catalysts [25].

3.6. Catalytic Activity

The methane conversion curves of the Pd/($Ce_{0.33}Zr_{0.66}O_2$)SiO_2 catalysts prepared with different Zr and Ce loadings are presented in **Figure 5**. The T_{20}, T_{50} and T_{100} values (respectively temperatures for 20%, 50% and 100% of methane conversion) (**Table 4**), decreased when the Zr loading increased from 0% to 4% and

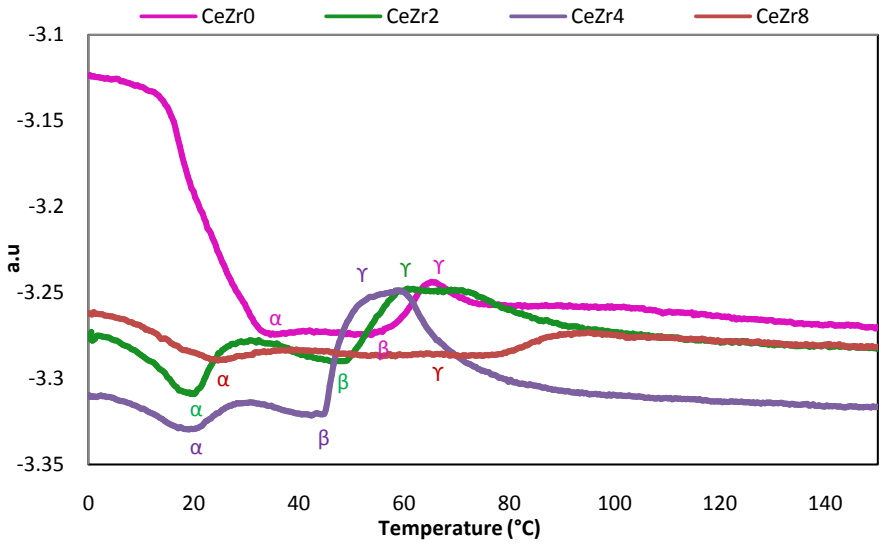

Figure 4. TPR profiles of the Pd/($Ce_{0.33}Zr_{0.66}O_2$)SiO_2 catalysts.

Table 3. Reduction temperatures of the Pd/($Ce_{0.33}Zr_{0.66}O_2$)SiO_2 catalysts.

Sample	T(˚C)	T(˚C)	T(˚C)
CeZr8	23	49	64
CeZr4	16	37	58
CeZr2	18	43	60
CeZr0	32	47	65

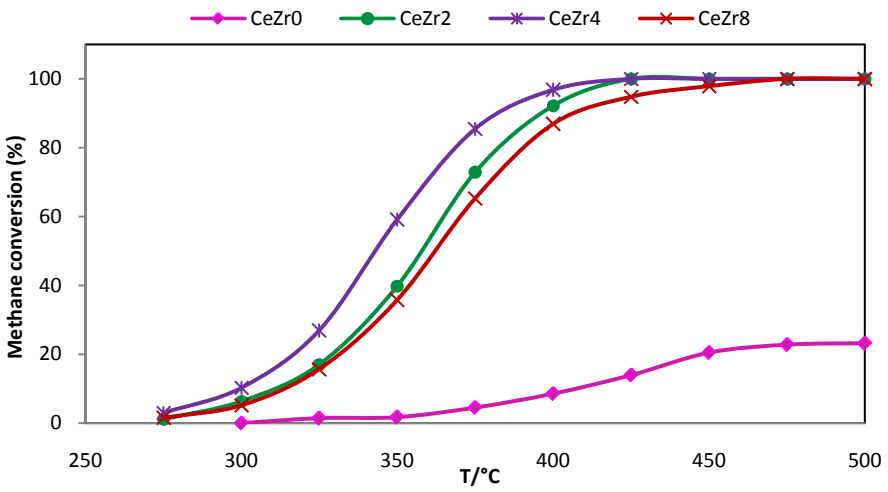

Figure 5. Effect of the Zr and Ce loadings on the activity of Pd/($Zr_{0.66}Ce_{0.33}O_2$)SiO_2 catalysts.

Table 4. Light-off temperature and turnover number at 325˚C of the Pd/($Ce_{0.33}Zr_{0.66}O_2$)SiO_2 catalysts.

Sample	T_{20}(˚C)	T_{50}(˚C)	T_{100}(˚C)	TOF[a](h^{-1})
CeZr8	331	362	462	875
CeZr4	317	342	415	1588
CeZr2	329	358	425	1243
CeZr0	450	-	-	157

[a]Turnover frequency (TOF) at 325˚C.

then increased with the further Zr loading increase to 8%. Thus the presence of cerium and zirconium oxides would obviously improve the thermal stability of PdO phase of the Pd/SiO_2 catalysts and enhance the catalytic activity. This is in agreement with our previous research. In fact, I. B. Said *et al.* [13] show that the addition of Ce and Zr to the Pd/MCM-41 enhance the catalytic activity for methane combustion, and an appropriate amount of these oxides can improve significantly its catalytic activity. In our case, this optimum corresponds to 4% of Zr and 3% of Ce. Considering the similar textural properties of CeZr4 and CeZr2 samples, the differences in the catalytic performance is mainly dependent on the reduction and structural properties. The TPR results show that improved

reducibility is obtained with increasing the doping amount of Zr in the following order: CeZr0 < CeZr2 < CeZr4. Furthermore these results suggest that the activity of the catalytic sites is enhanced by the improvement of the PdO reducibility. In addition, according to the XPS results, the increase in Zr and Ce amounts stabilizes palladium particles in PdO state and allows a strong interaction of PdO with the support, which enhances the re-oxidation properties of PdO.

Moreover, in the case of CeZr8 catalyst, the increase of Ce and Zr amount decrease the catalytic activity compared to that of CeZr4 and CeZr2 samples. As can be noted, similar dispersion and textural propriety are obtained for all catalysts. Thus, the reason how could mainly explain the activity drop is the Pd reducibility.

The turnover number frequency (TOF) has been calculated to investigate the effect of Ce and Zr introduction in the activity per site. As summarized in **Table 4**. it is clearly observed that the CeZr4 sample exhibit a relatively high TOF (1588 h^{-1}), in the combustion of methane at 325˚C, followed by CeZr2 (1243 h^{-1}), CeZr8 (875 h^{-1}) and CeZr0 (157 h^{-1}). From the obtained results, the TOF evolution can explain the activity decreases. The TOF is inversely proportional to the reduction temperature order. The higher the reduction temperature, the lower is the turnover number. As a conclusion, optimum values of Ce and Zr should be reached to maximize activity in methane combustion.

4. Conclusions

The following conclusions can be drawn from this work:

- The impregnation of the $(Ce_{0.33}Zr_{0.66}O_2)SiO_2$ aerogel support with palladium and the optimization of the Ce and Zr contents enable producing mesoporous $Pd/(Ce_{0.33}Zr_{0.66}O_2)SiO_2$ catalysts with relatively high specific surface areas;
- The palladium dispersion is improved when the Zr and Ce loading are increased on the $Pd/(Ce_{0.33}Zr_{0.66}O_2)SiO_2$ catalysts;
- With the preparation method adopted in this work, relatively small particles of CeO_2 and ZrO_2 oxides, are obtained on the $Pd/(Ce_{0.33}Zr_{0.66}O_2)SiO_2$ catalysts.
- The $Pd3d_{5/2}$ photopeak binding energy increased with the Ce and Zr amount increase. This seems to be due to a strong interaction between PdO and CeO_2-ZrO_2;
- The addition of Ce and Zr to Pd/SiO_2 (CeZr0) improves the PdO redox property and an optimum amounts of Zr and Ce is observed, for which the PdO reducibility is maximized; The improvement of the $Pd/(Ce_{0.33}Zr_{0.66}O_2)SiO_2$ reducibility is most likely responsible for the observed catalytic activity enhancement in the methane combustion reaction.

Acknowledgements

Chevreul Institute (FR 2638), Ministère de l'Enseignement Supérieur et de la Recherche, Région Nord-Pas de Calais and FEDER are acknowledged for supporting and funding partially this work.

References

[1] Liu, C., Xian, H., Jiang, Z., Wang, L., Zhang, J., Zheng, L., Tan, Y. and Li, X. (2015) Insight into the Improvement Effect of the Ce Doping into the SnO_2 Catalyst for the Catalytic Combustion of Methane. *Applied Catalysis B*: *Environmental*, **176-177**, 542-552.

[2] Di Iorio, S., Sementa, P. and Vaglieco, B.M. (2016) Analysis of Combustion of Methane and Hydrogen-Methane Blends in Small DI SI (Direct Injection Spark Ignition) Engine using Advanced Diagnostics. *Energy*, **108**, 99-107.

[3] Cao, L., Pan, L., Ni, C., Yuan, Z. and Wang, S. (2010) Autothermal Reforming of Methane over $Rh/Ce_{0.5}Zr_{0.5}O_2$ Catalyst: Effects of the Crystal Structure of the Supports. *Fuel Processing Technology*, **91**, 306-312. https://doi.org/10.1016/j.fuproc.2009.11.001

[4] Fan, X., Wang, F., Zhu, T. and He, H. (2012) Effects of Ce on Catalytic Combustion of Methane over $Pd\text{-}Pt/Al_2O_3$ Catalyst. *Journal of Environmental Sciences*, **24**, 507-511. https://doi.org/10.1016/S1001-0742(11)60798-5

[5] Fessi, S., Mamede, A.S., Ghorbel, A. and Rives, A. (2012) Sol-Gel Synthesis Combined with Solid-Solid Exchange Method, a New Alternative Process to Prepare Improved $Pd/SiO_2\text{-}Al_2O_3$ Catalysts for Methane Combustion. *Catalysis Communications*, **27**, 109-113. https://doi.org/10.1016/j.catcom.2012.06.016

[6] Okal, J., Zawadzki, M. and Baranowska, K. (2016) Methane Combustion over Bimetallic $Ru\text{-}Re/\gamma\text{-}Al_2O_3$ Catalysts: Effect of Re and Pretreatments. *Applied Catalysis B*: *Environmental*, **194**, 22-31.

[7] Gholami, R., Alyani, M. and Smith, K.J. (2015) Deactivation of Pd Catalysts by Water during Low Temperature Methane Oxidation Relevant to Natural Gas Vehicle Converters. *Catalysts*, **5**, 561-594. https://doi.org/10.3390/catal5020561

[8] Fan, X., Wang, F., Zhu, T.L. and He, H. (2012) Effects of Ce on Catalytic Combustion of Methane over $Pd\text{-}Pt/Al_2O_3$ Catalyst. *Journal of Environmental Sciences*, **24**, 507-511. https://doi.org/10.1016/S1001-0742(11)60798-5

[9] Zhou, Z.L., Ji, S.F., Yin, F.X., Lu, Z.X. and Li, C.Y. (2007) Preparation of $Pd/Ce_xZr_{1-x}O_2/SiO_2$ and Its Catalytic Performance in Methane Combustion. *Journal of Fuel Chemistry and Technology*, **35**, 583-588. https://doi.org/10.1016/S1872-5813(07)60035-8

[10] Ferrer, V., Finol, D., Rodríguez, D., Domínguez, F., Solano, R., Zárraga, J. and Sánchez, J. (2009) Chemical Characterization and Catalytic Activity of Pd-Supported Catalysts on $Ce_{0.39}Zr_{0.61}O_x/SiO_2$. *Catalysis Letters*, **132**, 292-298. https://doi.org/10.1007/s10562-009-0115-8

[11] Ruiz, J.A.C., Oliveira, E.C., Fraga, M.A. and Pastore, H.O. (2012) Performance of Pd Supported on Mesoporous Molecular Sieves on Methane Combustion. *Catalysis Communications*, **25**, 1-6. https://doi.org/10.1016/j.catcom.2012.04.006

[12] Kozlov, A., Kim, D., Yezerets, A., Andersen, P., Kung, H. and Kung, M. (2002) Oxidative Dehydrogenation of Alkanes over Vanadium-Magnesium-Oxides. *Journal of Catalysis*, **209**, 417-426. https://doi.org/10.1006/jcat.2002.3644

[13] Saïd, I.B., Sadouki, K., Masse, S., Coradin, T., Smiri, L. and Fessi, S. (2018) Advanced $Pd/CexZr_{(1-x)}O_2$/MCM-41 Catalysts for Methane Combustion: Effect of the Zirconium and Cerium Loadings. *Microporous and Mesoporous Materials*, **260**, 93-101. https://doi.org/10.1016/j.micromeso.2016.10.044

[14] Satterfield, C. (1980) Heterogeneus Catalysis in Practice. McGraw Hill, New York, 93.

[15] Graham, G.W., Schmitz, P.J., Usmen, R.K. and McCabe, R.W. (1993) Investigation of La^{3+}-Modified Al_2O_3 Supported CeO_2. *Catalysis Letters*, **17**, 175-184. https://doi.org/10.1007/BF00763940

[16] Vidmar, P., Fornasiero, P., Kaspar, J., Gubitosa, G. and Graziani, M. (1997) Effects of Trivalent Dopants on the Redox Properties of $Ce_{0.6}Zr_{0.4}O_2$ Mixed Oxide. *Journal of Catalysis*, **171**, 160-168. https://doi.org/10.1006/jcat.1997.1784

[17] Wang, X., Lu, G., Guo, Y., Qiao, D., Zhang, Z., Guo, Y. and Li, C. (2008) Properties of CeO_2-ZrO_2 Solid Solution Supported on Si-Modified Alumina and Its Application in Pd Catalyst for Methane Combustion. *Chinese Journal of Catalysis*, **29**, 1043-1050. https://doi.org/10.1016/S1872-2067(08)60081-9

[18] Yin, F., Ji, S., Wu, P., Zhao, F. and Li, C. (2008) Deactivation Behavior of Pd-Based SBA-15 Mesoporous Silica Catalysts for the Catalytic Combustion of Methane. *Journal of Catalysis*, **257**, 108-116. https://doi.org/10.1016/j.jcat.2008.04.010

[19] Wang, G., You, R. and Meng, M. (2013) An Optimized Highly Active and Thermo-Stable Oxidation Catalyst Pd/Ce-Zr-Y/Al_2O_3 Calcined at Superhigh Temperature and Used for C_3H_8 Total Oxidation. *Fuel*, **103**, 799-804. https://doi.org/10.1016/j.fuel.2012.08.051

[20] Yuan, Y., Wang, Z., An, H., Xue, W. and Wang, Y. (2015) Oxidative Carbonylation of Phenol with a Pd-O/CeO_2-Nanotube Catalyst. *Chinese Journal of Catalysis*, **36**, 1142-1154. https://doi.org/10.1016/S1872-2067(14)60312-0

[21] Kim, Y.T., You, S.J. and Park, E.D. (2012) Water-Gas Shift Reaction over Pt and Pt-CeO_x Supported on $CexZr_{1-x}O_2$. *International Journal of Hydrogen Energy*, **37**, 1465-1474. https://doi.org/10.1016/j.ijhydene.2011.10.014

[22] Ciuparu, D., Pfefferle, L.D. and Datye, A. (2002) Catalytic Combustion of Methane over Palladium-Based Catalysts. *Catalysis Reviews—Science and Engineering*, **44**, 593-649. https://doi.org/10.1081/CR-120015482

[23] Zhao, B., Yang, C., Wang, Q., Li, G. and Zhou, R. (2010) Influence of Thermal Treatment on Catalytic Performance of Pd/(Ce,Zr)O_x-Al_2O_3 Three-Way Catalysts. *Journal of Alloys and Compounds*, **494**, 340-346. https://doi.org/10.1016/j.jallcom.2010.01.031

[24] Zhou, Z.-L., Ji, S.-F., Yin, F.-X., Lu, Z.-X. and Li, C.-Y. (2007) Preparation of Pd/$Ce_xZr_{1-x}O_2$/SiO_2 and Its Catalytic Performance in Methane Combustion. *Journal of Fuel Chemistry and Technology*, **35**, 583-588. https://doi.org/10.1016/S1872-5813(07)60035-8

[25] Xie, S., Liu, Y., Deng, J., Zhao, X., Yang, J., Zhang, K., Han, Z. and Dai, H. (2016) Three-Dimensionally Ordered Macroporous CeO_2-Supported Pd@Co Nanoparticles: Highly Active Catalysts for Methane Oxidation. *Journal of Catalysis*, **342**, 17-26. https://doi.org/10.1016/j.jcat.2016.07.003